Comparison of Fundamental Mesh Smoothing Algorithms for Medical Surface Models

Ragnar Bade, Jens Haase, Bernhard Preim*
University of Magdeburg
{bade|preim}@isg.cs.uni-magdeburg.de

Abstract

For diagnosis, intervention planning, and medical education it is common to extract surface models from clinical tomography data. Surface extraction suffers from various effects of medical imaging, segmentation, and surface extraction techniques which cause visual disturbing surface artifacts (e.g. stairs, plateaus). Basic mesh smoothing algorithms for such surface models are a common feature of visualization toolkits. However, there exists no study concerning efficiency, accuracy, and appropriateness of different smoothing strategies for surface models derived from medical volume data.

To enable an elaborated and target oriented smoothing of medical surface models, we analyze and compare fundamental mesh smoothing algorithms applied to medical surface models. Based on the analysis of artifact sources and the classification of frequent object types that may make different demands on smoothing, we present smoothing recommendations for medical surface models.

1 Introduction

The extraction and visualization of surface models from medical volume data (e.g. CT, MRI) is supported by any clinical workstation and medical visualization software. Relevant regions and structures in image space are transformed into polygonal surface models for efficient and clear visualization. To transform structures in volume data into surface models, they have to be identified by their values (e.g. bones >1000 HU in CT) or by appropriate preprocessing and segmentation usually resulting in a binary segmentation mask. According to this mask, polygonal meshes (mostly triangle meshes) are created which represent the border surface of the desired structures in 3d space. In medical applications, accuracy, volume preservation (e.g. of pathological structures), and the conservation of distances between different surfaces is crucial. Fig. 1 shows (a) a slice of a MRI data set of the upper arm bone humerus, (b) the extracted surface model, and (c) a photograph of a humerus. Due to slice-based discrete sampling and physical conditions of medical imaging, extracted surface models suffer from artifacts and thus only represent an approximation of the real patient anatomy. As shown in Fig. 1 (b) and (c), an extracted surface model can strongly deviate from the real object. Missing or additional artificial object parts as well as frayed parts, holes, stairs and plateaus are frequent artifacts. The human visual system
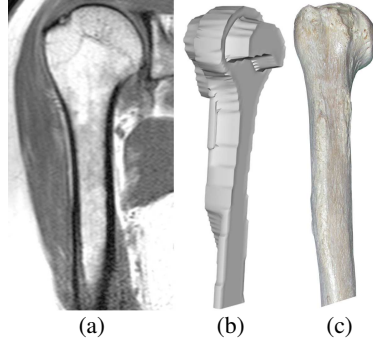

(a)   (b)   (c)

Figure 1: Example of MRI slice of upper arm bone humerus (a), extracted surface (by Marching Cubes) (b) and photograph of a humerus (c) (photograph source: [Wik05]).

is very sensitive to such discontinuities, since they normally represent important features for object detection and classification. Furthermore, such artifacts will be emphasized if feature enhancing visualization techniques (e.g. silhouettes, hatching, . . .) are used. As a consequence, such artifacts attract visual attention and distract from, hide, or even deface the original appearance of objects.

During the surface extraction process, these artifacts can be treated and reduced at the voxel level and at the surface mesh level (see Fig. 2). Methods operating at the voxel level perform subvoxel resampling, use non-binary segmentation masks or apply segmentation with subvoxel accuracy [SZH98]. Other methods smooth the binary segmentation mask [NFW+04] or perform a grey value dependent adjustment of contour borders during the mesh extraction phase [BVP+00]. At the mesh level, usually smoothing of the extracted surface meshes is performed to improve the surface extraction results. For this reason, basic mesh smoothing algorithms are part of common visualization software. However, considering the specific requirements and challenges for medical visualization, it is not yet clear which mesh smoothing algorithms are appropriate for medical visualization and how different parametrization of common smoothing algorithms affect the results. As a consequence, an elaborated and target oriented smoothing of medical surface meshes in consideration of the specific requirements on volume preservation and conservation of spatial extensions and relations, is not possible yet. To accomplish these goals, we investigate fundamental algorithms and strategies for smoothing medical surface models at the mesh level. In this framework, we compare the Laplace, Laplace+HC, and LowPass mesh smoothing algorithms. Based on the analysis of artifact sources and the classification of different object
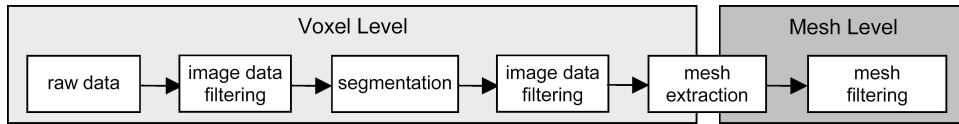

Figure 2: Surface extraction pipeline, cuts roughly into a voxel level and a mesh level.

2

types that make specific demands on the smoothing process, we derive recommendations for the smoothing of medical surface models.

2 Related Work

Previous work on smoothing polygonal surface models is predominantly related to technical models and deals with smoothing of arbitrary noise added to perfect surface models respectively [BO03, DMSB99, VMM99, YOB02]. As a consequence, in these studies smoothing algorithms with empirically adjusted parameters for the specific object are applied to draw conclusions concerning the accuracy of smoothing results in comparison to the (perfect) original model. Other studies only compare visual results and do not quantitatively evaluate the resulting surfaces [DMSB99, Tau95]. Comparative surveys e.g. [BO03] and [YOB02] only compare the deviation of the smoothing results of different algorithms with fixed parameters and increasing number of iterations with respect to the perfect original model. Recommendations to determine appropriate parameters are vague and restricted to some empirical values for the studied objects.

3 Problem Analysis

In order to systematically compare mesh smoothing algorithms and strategies for medical visualizations, we first analyze the cause of artifacts that make smoothing of extracted surfaces from medical volume data necessary or that hamper this process. We take each step of the surface extraction process beginning with the raw volume data up to the mesh extraction step (see Fig. 2) into account, to analyze possible problems and artifact sources. Moreover, we analyze the different surface models in medical visualizations according to their properties and specific characteristics and suggest an appropriate classification scheme. From these findings, we derive requirements for mesh smoothing for medical visualizations as well as criteria for the assessment of the smoothing results.

3.1 Artifact Sources in the Surface Extraction Process

Surfaces extracted from medical volume data result from a multi-level generation process consisting of the original object, image acquisition, segmentation, and mesh extraction. Since each step is a potential source for artifacts of the extracted surfaces, we analyze and discuss all artifact sources from each step.

3.1.1 Image Acquisition

Medical image acquisition techniques (e.g. CT, MRI) create discrete, equidistant, cross-sectional images with discrete sample points in each slice image. Common resolutions vary from 128x128x64 to 512x512x400, whereas the resolution in z-direction (inter slice) is commonly lower than in the x- and y-direction (intra slice).

Due to technical and physical circumstances, most images suffer from noise. Improvements of the signal-to-noise ratio during image acquisition are heavily restricted by the X-ray dose during a CT scan and by device-related costs of MRI.

The discrete resolution of the image acquisition techniques results in the so called partial volume effect. It describes the phenomenon of merging different density values of several tissues that are all together covered by one voxel or that are only partially covered (as illustrated in Fig. 3(a)). In the case of fine structures or sharp corners inside a volume element density values may be sampled that do not correspond to one of the actually present objects. As a consequence, sharp corners can get blurred and during the segmentation step such voxel can be assigned to a wrong or no object.

Since in clinical routine medical imaging is applied to patients, additional motion artifacts may occur e.g. caused by respiration. Furthermore, signal artifacts can occur, due to implants that block out the X-ray beams during CT scans or that provoke inhomogeneities in the magnetic field under MRI (see Fig. 3(b)).

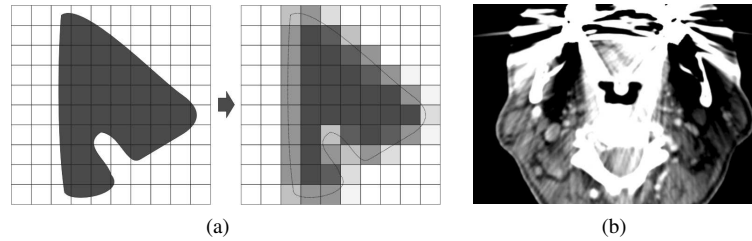<center>(a)   (b)</center>

Figure 3: Examples of image acquisition artifacts: (a) original object (left) and discrete sampled object (right) suffering from the partial volume effect; (c) CT-slice of the neck region suffering from heavy signal artifacts due to dental fillings and inlays.

3.1.2 Segmentation

During the segmentation process, each voxel of the volume data is classified as part of a specific object or as part of the background. This can be accomplished by simple thresholding techniques or other more flexible techniques. Regardless of the segmentation technique, the typical result is a binary classification (1 = part of the object, 0 = background) of all voxel. This can result in block artifacts, since each voxel is completely identified as being or not being part of an object. Furthermore, it is common to perform slice-based segmentation (e.g. LiveWire). As a consequence, the segmentation result is not necessarily consistent from one slice to another.

Moreover, segmentation can fail, due to artifacts of the image acquisition process. Blurry object borders (for example due to the partial volume effect and motion artifacts) or incorrect voxel values (e.g. due to noise and signal artifacts) can result in too many voxel that are classified as being part of an object (over-segmentation) or too few voxel (under-segmentation). This can lead to holes and frayed object parts as well as to additional or detached object parts at critical regions (e.g. thin object parts) (see Fig. 4).

frayed parts   additional/detached parts   holes

Figure 4: Example of a segmentation result suffering from frayed parts, holes, additional and detached parts.

3.1.3 Mesh Extraction

For surface mesh extraction from segmented volume data, often the Marching Cubes algorithm or accelerated modifications are used. They operate on cells composed of eight voxel and test for each cell whether the desired surface intersects this cell or not. If the desired surface intersects the cell, then the intersection points at the cell borders are calculated by linear interpolation. Finally, the gathered intersection points are connected to triangles inside of these cells. As a consequence of linear interpolation, sharp artificial edges in the extracted surface model can evolve or are retained from segmentation. Furthermore, by this method up to four triangles are created within each cell. Thus, resulting surface models usually contain a huge amount of small triangles. The huge amount of triangles slows down the runtime of the smoothing algorithms. The size of the triangles in relation to the size of surface features and artifacts (*triangle-size-to-feature-size ratio*) may slow down the smoothing process and accelerate the volume shrinkage respectively. We will regard to this later when we analyze different object types and their specific properties for medical visualizations.

Additionally, due to the typically lower resolution of medical volume data in the z-direction, small elongated triangles are created. This may interfere with the results of distance-weighted smoothing algorithms. Visible consequences are salient block and staircase artifacts in the z-direction.

3.1.4 Summary

Relevant artifacts from the image acquisition step are: (1) noise, (2) partial volume effect and (3) motion and signal artifacts; from the segmentation step: (4) block/staircase artifacts and (5) holes, (6) frayed parts and (7) additional/detached parts (e.g. caused by over- or under-segmentation); from the surface mesh extraction step: (8) salient/artificial surface edges, (9) huge amount of triangles, (10) small/large triangle size in relation to feature size as well as (11) elongated triangles.

The list contains even artifacts (e.g. motion and signal artifacts) that will not be reduced or eliminated by smoothing. However, appropriate smoothing algorithms should cope with imperfect data and should not amplify theses artifacts.

3.2 Object Analysis and Classification

Three-dimensional surface models of anatomical structures commonly exhibit no rectangular, sharp or straight-lined edges. They represent organic structures with smooth and often object specific furrows, branches, bulges, or indentations. This is different to models used in research on feature preserving smoothing algorithms as they are necessary in CAD/CAM applications. As a consequence, algorithms that are developed to preserve feature edges and to smooth technical objects will fail smoothing organic objects.

Furthermore, surface models of anatomical structures show a huge variety of different object features and characteristics. Since differently shaped objects behave differently while smoothing and different smoothing strategies are appropriate for different objects, it is reasonable to derive different object classes according to specific object characteristics. Hence, we classify all objects as compact, flat, or elongated (see Fig. 5). Furthermore, we distinguish objects according to their triangle-size-to-feature-size ratio. In this framework, we define objects as huge, if the triangle size is much smaller than the feature size and objects as small, if it is inversely related. We analyze characteristic features and problems of the different object classes and explain them in detail in the following sections.
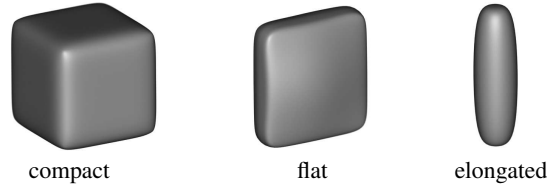

compact   flat   elongated

Figure 5: Object classification into compact, flat, and elongated objects.

3.2.1 Compact Objects

Compact objects are characterized by a relatively large volume in relation to a small surface area. Typical medical examples are liver, milt, kidneys, as well as small structures like lymph nodes and several glands. Typically the exact spatial location, volume, and extents of small compact objects (e.g. tumors and potentially pathological lymph nodes) are of medical relevance. In contrast, small deviations from the exact volume as well as moderate shrinkage of small object parts are acceptable for huge compact objects (e.g. organs).

Compact objects suffer mainly from block and staircase artifacts that can deface the original object e.g. by unnatural artificial edges. Furthermore, it is very likely that the size of a compact object in one slice diverges strongly from its size in the adjacent slices. At those regions, often staircase artifacts with large elongated stairs (so called plateaus) occur. Caused by the mesh extraction technique, at these plateaus a huge number of coplanar polygons is created that can hamper the smoothing process. Some compact objects can also contain detached object parts (e.g. satellites of a tumor or segmentation artifacts). Fig. 6 shows typical compact anatomical structures with the described artifacts. In contrast to larger objects, small compact objects like the lymph node in Fig. 6(c) exhibit regions of increased curva-
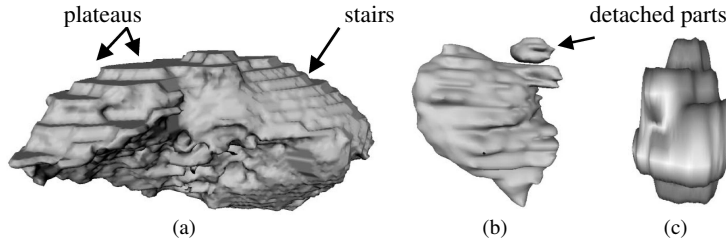
6

Figure 6: Examples for compact objects and their typical artifacts: (a) liver with plateaus and staircase artifacts; (b) tumor with detached parts (satellite); (c) enlarged model of a lymph node.

ture values and differences between adjacent triangles. This can result in heavy changes of the surface even by a small number of smoothing iterations and a small weighting factor.

3.2.2 Flat Objects

Objects are classified as flat, if their extension in one direction is considerably smaller than in the other directions. Typical examples are the neck muscle (*M. sternocleidomastoideus*) and bones like shoulder blades, breastbone, and the pelvis. Due to the partial volume effect, binary segmentation, and their small extent in one direction, it is very likely that corresponding extracted surface models suffer from frayed parts, holes, additional and detached parts. Caused by increased curvature and larger differences between adjacent triangles at these problem areas, smoothing can result in heavy deformation of these surface parts. Similar to compact objects, flat objects also suffer from block and staircase artifacts. Fig. 7 illustrates the discussed artifacts of flat objects. In addition, bended flat objects rise fur-
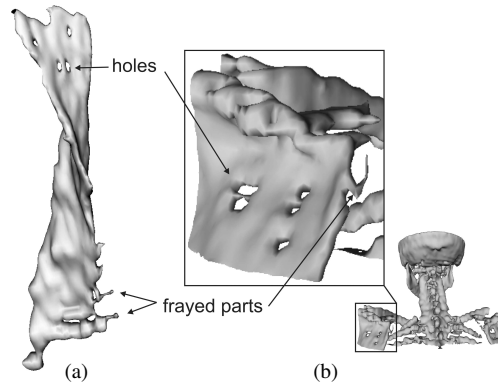

Figure 7: Examples for flat objects and their typical artifacts: (a) muscle of the neck region (*M. sternocleidomastoideus*) and (b) shoulder blade both with holes and frayed parts.

ther problems, since such structures tend to shrink in size, shape and position towards their center of mass. This can lead to serious changes of spatial distances and relations between surrounding objects.

3.2.3 Elongated Objects

Structures that mainly extend in one direction (along one possible bended axis) are classified as elongated objects. Blood vessels, bronchial tree, bones of the arm and legs, as well as the ribs are typical medical examples (see Fig. 8).

This object class mainly consists of small and filigree structures (e.g. vascular structures), whose continuous course and connectivity is important for their function (e.g. as pipelines). Due to their unfavorable triangle-size-to-feature-size ratio, most objects of this class heavily suffer from block and staircase artifacts as well as from negative side effects of smoothing methods. For example, staircase artifacts can lead here to visually distracting and diagnostic misleading constrictions. Furthermore, it is likely that parts of such thin and filigree objects are not exactly represented in different slices due to the partial volume effect. As a consequence, an increased number of disconnected object parts can be generated during mesh extraction.

Elongated objects can also exhibit several branches whose existence, number, and branching behavior is important. Smoothing algorithms can distort these branchings as well as shrink and collapse thin object parts that can lead to further distortions and detached object parts.
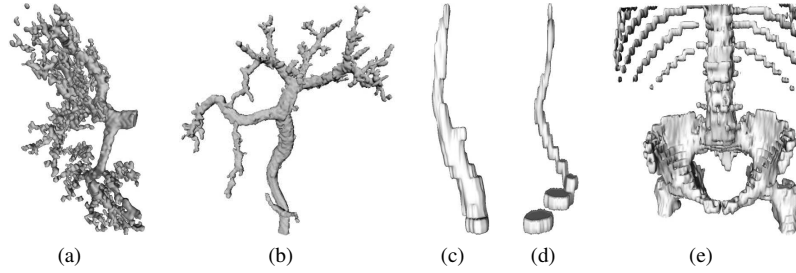

(a) (b) (c) (d) (e)

Figure 8: Examples for elongated objects and their typical artifacts: (a) highly branched hepatic vascular tree with detached object parts, (b) hepatic vascular tree with a few branches, (c) carotid artery (*A. carotis*), (d) jugular vein *V. jugularis*, and (e) ribs in context of abdominal bones with heavy staircase artifacts and detached object parts.

3.3 Mesh Smoothing Requirements for Medical Visualizations

From the analysis of artifact sources and the specific characteristics of medical surface models, we derive requirements for mesh smoothing for medical visualizations.

The primary goal of mesh smoothing is to achieve (A) a visual improvement. To accomplish this goal, (A-1) block and staircase artifacts of all objects as well as (A-2) plateaus

(especially of compact objects) have to be reduced. For flat objects, primarily (A-3) closing holes and (A-4) reducing frayed parts is desirable. For elongated objects, it is worthwhile to restore their continuous shape by (A-5) reconstructing a continuous diameter distribution and (A-6) reconnecting detached object parts. According to the object class, deviations from the original are acceptable or should be avoided. To avoid deviations that exceed a defined value, (B) appropriate stop criteria are necessary. These should warrant (B-1) object specific feature preservation, (B-2) volume preservation, and (B-3) the conservation of spatial extensions and relations, as well as that (B-4) artifacts are not amplified.

3.4 Smoothing Result Assessment Criteria

To assess if a mesh smoothing strategy meets the requirements listed above, in this section we list and briefly analyze criteria that guarantee the assessment of quality and correctness to the original surface model.

Appropriate criteria to assess the visual improvement ($\uparrow$A) are: visual inspection, triangle quality, maximum curvature, as well as the change of the surface area under smoothing. The surface area can be easily used to evaluate the smoothing process since it shrinks while smoothing and it can be easily calculated or is even a part of some smoothing algorithms.

To assess the deviation or error according to the original model ($\uparrow$B) the volume, main axes extents, and distance measurements (e.g. the Hausdorff distance) are appropriate. The deviation or distance to the original can also be assessed by visual inspection of appropriate visualizations. Additional criteria of the appropriateness of a smoothing method are its calculation complexity and run time.

4 Comparison and Assessment Concept

To compare and assess smoothing methods and strategies, we developed a concept that can be applied in the routine of medical visualization. In this concept, the initial extracted surface model is referred to as the "original" and comparison and assessment is performed in relation to this imperfect and with artifacts afflicted original. This concept is geared to the medical visualization routine, where no "perfect" model of the correct patient individual anatomy is available. Thus, smoothing results and experiences from this study cannot only be used to derive smoothing recommendations but also to be directly integrated into the common visualization process (e.g. as stop criteria).

In this study, we used MeVisLab [MeV05] to implement the different smoothing algorithms and Amira [ZIB05] to analyze the smoothing results with respect to the before mentioned assessment criteria. In the next sections the used surface models and assessment criteria for this study as well as the smoothing algorithms and their parameters are briefly introduced.

4.1 Surface Models and Assessment Criteria

To compare the different smoothing algorithms, we apply them to six reference objects (two objects of each object class). The objects are chosen in such a manner that they represent typical objects of their class with typical features and artifacts (see Tab. 1). Among the

compact objects, we selected a surface model of a liver and a lymph node. Whereas both heavily suffer from block and staircase artifacts, the lymph node model in addition represents a small compact object with an unfavorable triangle-size-to-feature-size ratio. The flat object representatives are surface models of a neck muscle and of a pelvis. A heavily branched vascular tree with many small detached parts and a slightly thicker, none branched carotid artery are selected as representatives for elongated objects. To keep the comparison concise, we only use the distribution of the maximum curvature (max value of the two principal curvature values) as an indicator for the smoothness and as a numerical criterion to assess the visual improvement (↑A), as well as the symmetric Hausdorff distance (as a displacement measure) and the volume (as a measure of shrinkage) to assess the error (↑B) with respect to the original surface. Thus, these criteria are collected in each smoothing step of all reference objects with each algorithm. The maximum curvature is calculated for each vertex of the model and represented by the mean and standard deviation for the whole surface model. The maximal value of the symmetric Hausdorff distance of each vertex with respect to the original surface is used to represent the maximum distance/error to the original. In addition, the time required for smoothing (at a PC with a 3.2GHz Intel$^®$ Pentium$^®$ 4 Processor and 1GB RAM) is recorded.
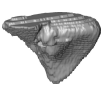
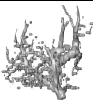## 4.2 Smoothing Algorithms and Parameters

In this study, we compare fundamental mesh smoothing algorithms that are commonly applied to medical surface models or that promise volume preservation. The smoothing algorithms and their parameters are briefly introduced in the next sections.

4.2.1 Laplace Mesh Smoothing Algorithm

The Laplace filter (also called *Laplacian Flow* or *Relaxation filter*) is the simplest mesh smoothing algorithm. It uses a direct topological neighborhood (see Fig. 9) and produces smooth meshes within a few iterations.
The Laplace filter iteratively traverses all surface vertices and moves each vertex into the geometric center of its topological neighbors. This procedure can be repeated iteratively

Table 1: Test objects used in this study and their properties.

	liver	lymph node	neck muscle	pelvis	vasculature	carotid artery
Faces	37 148	3 412	9 616	53 930	23 236	1 956
Vertices	18 576	1 708	4 804	27 211	11 820	982
Voxel	1 696 250	1 664	101 035	430 318	96 807	16 404

until the desired smoothness is achieved. Since this procedure strongly shrinks the surface model, often a weighting factor λ is introduced. This factor regulates the effect of the direct neighbors on the new position of the current vertex in each iteration. The new smoothed position p' of all vertices P results from its old position p and its neighbors q as shown in equation (1):

$$p' = p + \frac{\lambda}{n} \sum_{i=0}^{n-1} (q_i - p) \tag{1}$$

The Laplace filter with its two parameters (number of iterations and weighting factor λ) represents the most popular mesh smoothing method. This filter is equivalent to the *vtkSmoothPolyDataFilter* of the VTK, except that the VTK filter treats sharp and bounding edges separately [Kit05].

4.2.2 Laplace+HC Mesh Smoothing Algorithm

The Laplace+HC mesh smoothing algorithm, introduced by [VMM99] reduces shrinkage caused by the Laplace filter. The concept of the HC algorithm extension is that vertices moved by the Laplace filter are somewhat moved back to their former position. Direction and amount for this backward movement are derived from the original and previous vertex position as well as from the mean displacement vector in the neighborhood. Alternating execution of Laplace smoothing and HC algorithm results in a sufficient smoothing with no or low volume shrinkage.

Since the Laplace+HC filter is based on the Laplace filter, the Laplace+HC filter has the same two basic parameters plus two additional parameters for the HC algorithm. One of these additional parameters (α) regulates the effect of the original and previous vertex positions and the other (β) that of the displacement vectors in the neighborhood on the backward movement. To avoid to span a four dimensional search space for this filter, we restricted each additional parameter to a common fixed value. Inspired by [VMM99], we set $\alpha = 0$, so that all vertices are only moved back to their former positions and we set $\beta = 0.2$ so that the own displacement vector contributes with a factor of 0.2 and the mean displacement vector of the neighborhood with a factor of 0.8 to the backward movement.
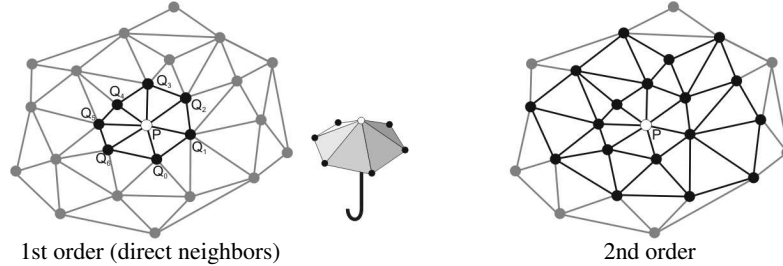

1st order (direct neighbors)   2nd order

Figure 9: Topological neighborhood (*umbrella region*) of polygonal meshes.

11

4.2.3 LowPass Mesh Smoothing Algorithm

The LowPass filter (also called $\lambda | \mu$ filter) [Tau95] represents a combination of two Laplace like filters, one with a positive weighting factor and one with a negative factor that are executed alternatingly. The new position p' of all vertices P results here from its old position p and its neighbors q as shown in equation (2):

$$p' = p + \lambda \sum_{i=0}^{n-1} \omega_i (q_i - p) \qquad (2)$$

For the LowPass filter, the weighting factor ω is commonly set to $1/n$ [Tau95], with the result that this filter is equivalent to the Laplace filter. In contrast to the Laplace filter, with the LowPass filter first a standard Laplace smoothing with an arbitrary weighting factor λ is applied and in the second step, the Laplace filter is applied again but now λ is replaced by μ while μ is set to a value a little bit smaller than $-\lambda$. Thus, similar to the Laplace+HC filter, a smoothing step and a backward moving step are alternately executed that much better preserves the volume than the Laplace filter.

In contrast to the Laplace filter, this filter has an additional parameter μ. To enable a comparison to the filters introduced before, μ is set to $\mu = -1.02\lambda$ as inspired by [Tau95].

In the VTK, the *vtkWindowedSincPolyDataFilter* represents an equivalent of the LowPass filter, except that the VTK filter again treats sharp and bounding edges separately [Kit05].

4.3 Comparison Procedure

Most previous comparative studies only compare smoothing algorithms with empirically chosen fixed parameters which are not studied in detail. In contrast, comparison of smoothing algorithms with alterable parameters is much more complex but necessary for an appropriate comparison of achievable smoothing results. Hence, we compare the discussed smoothing methods each with a 1st and 2nd order neighborhood, four different iteration steps (5; 10; 20; 50) and six different weighting factors (0,05; 0,1; 0,3; 0,5; 0,7; 0,9) applied to six representative surface models. This approach leads to (3 filter $\times$ 2 neighborhoods $\times$ 4 iteration steps $\times$ 6 weighting factors $\times$ 6 models) 864 interim smoothing results that have to be analyzed.

We first represent the smoothing results of the six reference objects in an iteration-step-by-weighting-factor matrix (one matrix per object). Then, these matrices of an object smoothed with different smoothing algorithms can be compared to each other. From these matrices then the best results can be identified. Furthermore, smoothing recommendations as well as stop criteria can be derived for the different artifacts and object classes in consideration of the resistance or disappearance of artifacts in relation to different smoothing methods and parameter combinations.

Since a presentation of all matrices is beyond the scope of the paper, only selected examples are included. For further reading all matrices can be found at [VIS06].

5 Results

In this section, we present and discuss the smoothing results of the different filters. We discuss each object class in detail and compare and summarize the results.

5.1 Smoothing Results of Compact Objects

For smoothing compact objects (e.g. liver, lymph nodes), the LowPass filter and the Laplace+HC with a weighting factor between 0.5 and 0.9 and with 20 to 50 iterations turned out to be equally appropriate. Here, the Laplace+HC filter is comparable to the LowPass filter with respect to the achieved visual improvement and error measures (see Tab. 2).

Smoothing with both filters and a 1st order neighborhood could not remove the heavy staircase artifacts and plateaus. With a 2nd order neighborhood these artifacts could be reduced much better, but the time required increased by a factor of 50 in our tests. The worst results were achieved with the Laplace filter, that yielded heavily shrunk surface models.

5.2 Smoothing Results of Flat Objects

The Laplace filter turned out to be the worst filter for smoothing flat objects and yielded heavily shrunk surface models as well. Again, smoothing with the LowPass and Laplace+HC filter yielded the best results. However, the LowPass filter slightly better preserves the volume and shape of frayed parts and holes (see Tab. 3). The best results can be achieved with a weighting factor between 0.5 and 0.7 and 20 iterations. Similar to the results for compact objects, smoothing flat objects with a 2nd order neighborhood reduces much better severe artifacts, but in contrast here a 2nd order neighborhood much more deforms frayed parts and holes.

5.3 Smoothing Results of Elongated Objects

Appropriate smoothing of heavily branched elongated objects with accessory detached parts (vascular tree) is not possible with one of the smoothing algorithms. They all yield heavy deformation and shrinkage of small and detached objects (see Tab. 4 left). Even low parameter values for smoothing cannot bee used, since they do not visually improve the surface models.

Only with the LowPass or Laplace+HC filter moderate smoothing of simple none branched elongated objects is possible (see Tab. 4 right). Once again, the LowPass filter better preserves the volume than the Laplace+HC. That also results in better distance values with respect to the original object. However, small objects or object parts with a small diameter shrink very fast, whereas bigger object parts tend to grow in size while smoothing with the LowPass filter. Best results could be achieved here with a weighting factor of 0.5 and 10 to maximal 20 iterations. Smoothing with a 2nd order neighborhood is not appropriate here, since small and detached parts shrink dramatically.

13

Table 2: Smoothing results of the liver surface model by means of different smoothing algorithms with a weighting factor of 0.9 and 50 iterations.
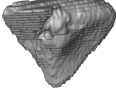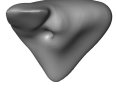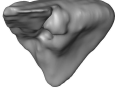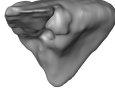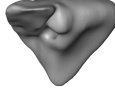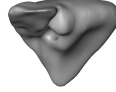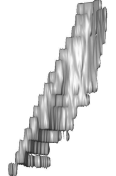
original	Laplace	Laplace+HC	LowPass	Laplace+HC 2nd order	LowPass 2nd order
V=100%	V=91.0% 2.03sec	V=99.9% 3.91sec	V=100.1% 4.36sec	V=99.6% 224.14sec	V=100.2% 220.95sec

Table 3: Smoothing results of the neck muscle model by means of different smoothing algorithms with a weighting factor of 0.5 and 10 iterations.
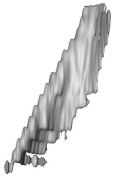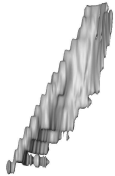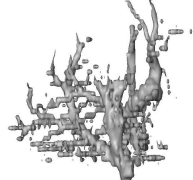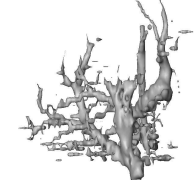
original	Laplace	Laplace+HC	LowPass	Laplace+HC 2nd order	LowPass 2nd order
V=100%	V=86.5% 0.11sec	V=100.0% 0.23sec	V=99.3% 0.25sec	V=94.4% 12.55sec	V=97.1% 11.97sec

Table 4: Smoothing results of elongated surface models.

original	LowPass weighting factor 0.5 iterations 10	original	LowPass weighting factor 0.7 iterations 10
V=100%	V=91.9% 0.61sec	V=100%	V=104.3% 0.05sec

6 Smoothing Recommendations

In our investigations, the LowPass filter turned out to be the most appropriate fundamental smoothing filter for all reference objects. To smooth compact objects, primarily the Low-Pass filter with a 2nd order neighborhood, a weighting factor of about 0.7, and 20 to 50 iterations should be used. A similar smoothing strategy can be applied to flat objects without or with a few frayed parts and holes, whereas here not more than 20 iterations should be applied. In contrast, flat objects with such problematic regions should be smoothed with a 1st order neighborhood. Elongated objects with many filigree branches and detached object parts cannot be smoothed appropriately with any of the tested filters. For smoothing vascular trees, model-based smoothing that somewhat abstracts from the real anatomy as presented in [OP05] tends to be the most promising procedure at least for visualizations not intended for diagnostic tasks. To smooth relatively simple and sparse or none branched elongated objects, the LowPass filter with a weighting factor of 0.5 and 10 iterations is recommended.

Assessment criteria that turned out to be potential stop criteria for assessing the visual improvement ($\uparrow$A) are the determination of the surface area and the distribution of the maximum curvature with mean and standard deviation. To assess the deviation/error of the smoothed surface in relation to the original surface model ($\uparrow$B), the symmetric Hausdorff distance and the volume of the model turned out to be appropriate. To employ the change of the volume as a stop criterion is not appropriate for elongated objects, since here at the same time small regions tend to shrink and others tend to grow in size. As a result, the whole object volume does not change, though the smoothing result heavily diverges from the original.

7 Conclusion and Discussion

Based on the presented analysis of artifacts, classification of objects into specific groups (compact, flat, elongated), and comparison of different parameter combinations of fundamental mesh smoothing algorithms, we are able to derive first smoothing recommendations for medical visualizations. Nevertheless, this study illustrates that smoothing of the extracted surface models visually improves the surfaces only to a limited extent. Frayed parts, holes, and detached parts predominantly represent none reducible artifacts by means of mesh smoothing.

Future work should analyze more sophisticated mesh smoothing methods and strategies (e.g. diffusion-based smoothing). Furthermore, methods that work at the voxel as well as the mesh level to achieve visual improvements are left open for further studies. Automatic smoothing of medical surface models is another important issue. In this context, automatic identification of the object type (e.g. compact, flat, elongated) and detection of artifacts should lead to an automatic determination of appropriate smoothing strategies and parameters.

References

[BO03]   A. Belyaev and Y. Ohtake. A comparison of mesh smoothing methods. In *Proc. Israel-Korea Bi-National Conference on Geometric Modeling and Computer Graphics*, pages 83–87, 2003.

[BVP⁺00]   P.W. Bruin, F. Vos, F.H. Post, et al. Improving triangle mesh quality with surfacenets. In *Proc. MICCAI'00*, pages 804–813, 2000.

[DMSB99]   M. Desburn, M. Meyer, P. Schröder, and A.H. Barr. Implicit fairing of irregular meshes using diffusion and curvature flow. In *Proc. Siggraph'99*, pages 317–324, 1999.

[Kit05]   Kitware Inc. Vtk 4.5.0 documentation. 1.2. http://www.vtk.org/doc/nightly ¬ /html, 2005. 04/16/2005.

[MeV05]   MeVis. Mevislab. http://www.mevislab.de, 2005. 10/10/2005.

[NFW⁺04]   A. Neubauer, M.-T. Forster, R. Wegenkittl, et al. Efficient display of background objects for virtual endsocopy using flexible first-hit ray casting. In *Proc. VisSym'04*, pages 301–310, 2004.

[OP05]   S. Oeltze and B. Preim. Visualization of vasculature with convolution surfaces. *IEEE Trans. Med. Imaging*, 24(4):540–548, 2005.

[SZH98]   D. Stalling, M. Zöckler, and H.-C. Hege. Segmentation of 3d medical images with subvoxel accuracy. In *Proc. CARS'98*, pages 137–142, 1998.

[Tau95]   G. Taubin. A signal processing approach to fair surface design. In *Proc. SIGGRAPH'95*, pages 351–358, 1995.

[VIS06]   VIS, University of Magdeburg. Comparison of mesh smoothing algorithms and strategies for medical surface models. http://wwwisg.cs.uni-magdeburg.de/cv/projects/LST/smoothing, 2006. 11/01/2006.

[VMM99]   J. Vollmer, R. Mencel, and H. Müller. Improved laplacian smoothing of noisy surface meshes. In *Proc. EuroGraphics'99*, pages 131–138, 1999.

[Wik05]   Wikimedia Foundation Inc. Wikipedia, the free encyclopedia. http://en.wikipedia.org/wiki/Humerus, 2005. 09/19/2005.

[YOB02]   H. Yagou, Y. Ohtake, and A.G. Belyaev. Mesh smoothing via mean and median filtering applied to face normals. In *Proc. Geometric Modeling and Processing*, pages 124–131, 2002.

[ZIB05]   ZIB, Mercury Computer Systems. Amira - advanced 3d visualization and volume modeling. version: 2005. http://www.amiravis.de, 2005. 06/09/2005.